Available online at www.sciencedirect.com

ScienceDirect

Procedia Structural Integrity 42 (2022) 236–243

Structural Integrity Procedia

www.elsevier.com/locate/procedia

23 European Conference on Fracture - ECF23

Reliability-based structural analysis of a bucket wheel excavator's load-bearing steel structure

Ana Petrović[a]*, Nikola Momčilović[b], Simon Sedmak[c]

[a]*University of Belgrade, Faculty of Mechanical Engineering, Kraljice Marije 16, Belgrade, Serbia*
[b]*University of Belgrade, Faculty of Mechanical Engineering, Kraljice Marije 16, Belgrade, Serbia*
[c]*Innovation Centre of Faculty of Mechanical Engineering, Kraljice Marije 16, Belgrade, Serbia*

Abstract

Structural analysis of large structures such as bucket wheel excavators (BWE) are generally performed using the finite element analysis and assessed according to the portion of the material's yielding limit. Consequently, a structure is evaluated just by the maximum stress at the specific location. In order to address the whole structural response of the object, this paper introduces a reliability-based structural evaluation presented on a case study of the BWE SchRs 630. Although the BWE reliability has been explored in literature, most of the research was based on data obtained from failure of systems and structure, over the years. Nevertheless, this investigation is dividing the pure structural from the system failure by mapping and analyzing the specific structural zones of the BWE. Finite element method obtained randomized stresses (i.e., D – demand of the structure) in a structure are categorized as independent variables and modeled using probability density function. The same is performed in case of the criterion – yield strength of the structure's material (i.e., C – capacity of the structure). Furthermore, yield strength distribution itself is evaluated according to the industry's practice meaning that mean value of the yield stress is to be reduced when used as a criterion for the stress assessments. Therefore, a margin function is analyzed according to the equation: M = C – D. Consequently, the structure is assessed as a whole through the introduction of the reliability index based on stresses. Such evaluation could enable comparison between the corresponding and similar structures in terms their structural response in more holistic manner.

Keywords: bucket wheel excavator SchRs 630; structural reliability; reliability index based on stress

* Corresponding author. Tel.: +381 69 2308888; fax: /.
E-mail address: aspetrovic@mas.bg.ac.rs

10.1016/j.prostr.2022.12.029

1. Introduction

In practice, large steel structures are generally evaluated using stresses obtained from linear elastic (or nonlinear) analysis and compared to the criterion based on design codes of the industry. Therefore, stresses are calculated based on theory of elasticity for beams or plates and in more sophisticated manner – using finite element method. Design criterion is mostly attributed on the yield stress limit of the material along with corresponding reduction factor acting as a safety zone. The data used in such evaluation are deterministic in its nature. Thus, the whole structure is evaluated using just one value (maximum stress) and confronted to another single value (yield stress), while not addressing the overall complexity of the global response and uncertainties.

Reliability-based structural analysis expands the assessment by including uncertainties into the probabilistic approach, see more on theoretical background in reference by Melchers and Beck (2018) and Wang (2021), as well as in Kovač et al (2022), Ngyen and Le (2019), Sedmak et al (2016), Kalaba et al (2016), Kalaba et al (2015), Ristić and Ognjanović (2014), Novoselac et al (2014), Szavai and Koves (2010) for practical applications. Variables are not deterministic as in case of classical approach, but stochastic with their own probability distributions. Therefore, in order to investigate reliability analysis of large steel structures, this paper introduces such approach in the case study performed on a bucket wheel excavator's (BWE) load-bearing steel structure, chosen due to its complexity, size and importance. BWE is the first machine in the chain of surface coal mining, so it follows, the number of failures of these machines should be reduced to zero, as elaborated in the following references: Arsić et al (2021), Daničić et al (2013), Daničić and Maneski (2012), Daničić et al (2010), Tanasijević et al (2010), Polovina et al (2010), Arsić et al (2008), Bošnjak et al (2005), Maneski and Ignjatović (2004).

Indeed, BWEs have been analyzed using reliability methods. Most of the research included mechanical and system failures based on an already given historical data from the exploitation or analysis performed on a specific part of the BWE, see reference by Lazarević et al. (2018), Lazarević et al (2015) and Tomus et al. (2019). However, this paper is separating the mechanical or system failures form the structural ones. Goal of this analysis is to assess the "pure" structural reliability of BWE using both stresses and respective criterion with their own uncertainties. This could address the overall structural "health" of the object, called here – structural reliability.

Nomenclature

C	capacity of the structure (σ_{all})
D	demand of the structure (σ_{VM})
$f(\sigma_{VM},\sigma_{all})$	joint probability density function
M	margin
n	numbers of variables (total or less than total)
N	total number of variables
pdf(X)	probability density function of random variable X
P_f	probability of failure
R	reliability
RF	reduction factor of the yield stress limit
SM	safety margin
X	random variable (σ_{VM} or σ_{all})
β	reliability index
μ	mean value
μ_N	mean value of normally distributed ln(X)
ρ	correlation coefficient
σ	standard deviation
σ_{all}	allowable stress (portion of the σ_y)
$\sigma_{all,\,max}$	max allowable stress according to the distribution range
$\sigma_{all,\,min}$	min allowable stress according to the distribution range
σ_{VM}	Von Mises stress [MPa]
σ_y	yield limit stress [MPa]

2. Structural model

Bucket wheel excavator SchRs 630 is already presented in reference by Petrović et al. (2021). Structural response calculation is performed for the one typical type of loading condition in which the structure is subjected most of the service life. Loading condition is considering as fully loaded and include steel weight of the structure and working loads (vertical, lateral and frontal force representing overall digging force). Such model is assessed using finite element method software KOMIPS developed at the Department of the Strength of Structures of the Faculty of the Mechanical Engineering (University of Belgrade) by Maneski (1998). The analysis type is linear-elastic regarding the material behavior. Steel structure is made of steel S355J2G3, and modulus of elasticity used in calculations is 210 GPa. Von Mises stress field is shown in Fig. 1 (in kN/cm^2, as in software produced), while the acquired Von Mises stresses at specific locations are presented in Table 1 in MPa (MPa will be used from now on as a unit for stress). The choice of locations of acquired stresses is explained in the following section.

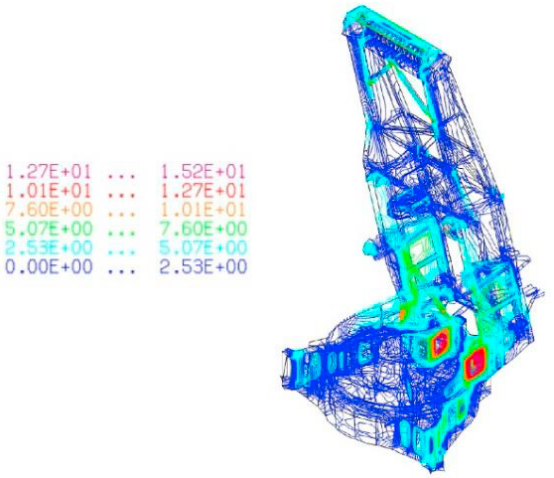

Fig. 1. Von Mises Stresses, in kN/cm^2, load bearing steel structure of BWE SchRS 630

The choice of locations of acquired stresses is based on function of structural elements. Basically, there are three units: undercarriage (Fig. 2. (a)), slewing platform (Fig. 2. (b)) and pylons (Fig. 2. (c)). Undercarriage and slewing platform are connected using axial bearing. Both, undercarriage and slewing platform contain two horizontal plates connected with two cylinders and radial vertical plates. So, decision is made to map the model in following way: on every plate zones of stress concentration are mapped, along with additional zone in the rest of the plate. So, lower plate of undercarriage is mapped in five locations: stress concentration in the zone of vertical plates under pylons, left and right (location 1 and 4), stress concentration in the zone of back support, left and right (location 3 and 5), and the rest of the plate (location 2), as shown in Fig. 2. (d). The same mapping is applied to upper plate od undercarriage (location 6 to 10).

Vertical plates of undercarriage are mapped in the same way: zone of stress concentration under pylons, left and right (location 11 and 12), vertical plates in the zone of back support (location 13 and 14), and the rest of the plate (location 15), as shown in Fig. 2. (a). Three locations on the external cylinder of undercarriage are mapped (location 16, 17 and 18). Considering the same strategy in mapping of slewing platform, three zones by each horizontal plate are noticed (location 19 to 24), five zones on vertical plates (location 25 to 29), and two zones on external cylinder (location 30 to 32), and some of them are shown in Fig. 2. (b).

Construction of pylons is divided in six zones, left and right (location 33 to 44), in which representative (maximum) stress is read. For instance, location 33 is on the right pylon in the lowest zone of pylons, and location 34 is on the left pylon in the same zone, Fig. 2. (c). So, location 35 is on the right pylon in second lowest zone, and location 36 is on the left pylon in the same zone, etc. Location 45 to 48 are parts of pylon vertical truss and are also marked in Fig. 2. (c) (except location 46, connection of sprit to the right pylon). Location 49 and 50 are locations on the top of the pylons, 49 is location where pulleys are connected to pylons.

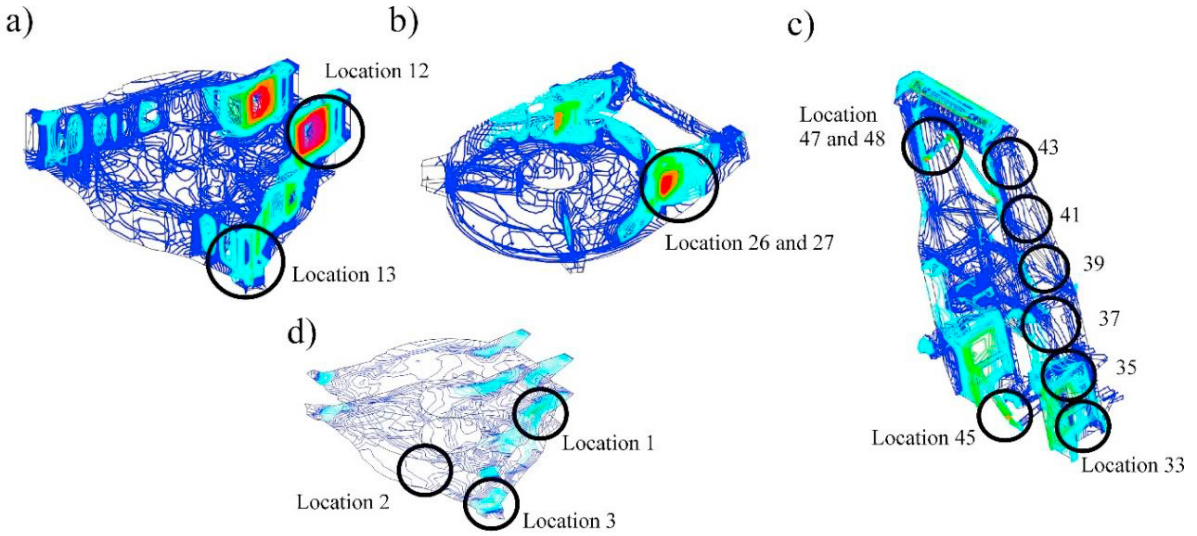

Fig. 2. (a) Locations of interest, Von Mises Stresses, undercarriage, (b) Locations of interest, Von Mises Stresses, slewing platform, (c) Locations of interest, Von Mises Stresses, pylons, (d) Locations of interest, Von Mises Stresses horizontal plates of undercarriage

Table 1. Von Mises stress results at positions.

Location	σ_{VM} [MPa]	Location	σ_{VM} [MPa]	Location	σ_{VM} [MPa]	Location	σ_{VM} [MPa]
1	50.40	14	55.65	27	73.12	40	19.66
2	27.79	15	27.23	28	60.26	41	35.30
3	56.56	16	89.60	29	28.78	42	43.47
4	39.95	17	57.02	30	73.10	43	53.42
5	55.03	18	24.97	31	64.54	44	53.77
6	60.83	19	51.58	32	20.30	45	101.00
7	26.38	20	44.62	33	68.12	46	187.50
8	58.62	21	14.30	34	67.29	47	184.50
9	51.19	22	73.74	35	33.43	48	95.49
10	62.77	23	88.19	36	28.56	49	84.69
11	130.30	24	23.20	37	27.65	50	3.20
12	161.90	25	111.10	38	18.14		
13	74.72	26	141.30	39	19.89		

3. Probability models

Probability and reliability theory used in this paper is thoroughly explained in reference by Melchers and Beck (2018), Wang (2021) and O'Connor and al. (2016). Somewhat the same principle used in this paper is also applied in case of reliability analysis of large steel hull, as presented by Motok and al. (2022). Here, the idea was to model the actual demand (D) and the capacity of the structure (C) in a form of probability density functions (pdf), so that the margin function (M) is the limit state function, defined in eq. (1):

$$M = C - D \tag{1}$$

Here, a demand is loading, i.e., Von Mises stress of the structure, while the capacity of the structure is represented by yield limit of the material (criterion). So, in order for the structure to be safe, the capacity of the structure has to be larger than its demand in all conditions ($M > 0$). If the capacity is lower than the demand ($M < 0$), than the structure is considered as failed. Since the uncertainties of both capacity and demand are included in the analyses, the failure comes with a certain probability.

3.1. Stresses

Using probability approach, Von Mises stresses (Table 1) are modeled as a group of independent variables conducted from the finite element analysis. They are acquired from the various specific locations (50 in total) of the mapped structure. Mapping is executed on its characteristic geometrical locations and dispersed semi-arbitrarily to include all the spots that can reliably describe the whole object's response. Locations certainly include maximum stress spots and areas where the potential structural failure could cause major consequences independently on the actual magnitude of stresses and loading. Moreover, the authors varied the reduction factor of the criterion (yield limit) in order to evaluate its effect on the reliability of the structure. Based on Table 1, a histogram is created in Fig. 4. (a), where a frequency of stress occurrence is plotted against their discrete range. Note that a negative stress value is not existing in the model since all the results are acquired in absolute value. Most of the stresses in structure are grouped in 45-65 MPa range, while a long right tail is showing the extremes.

For the purpose of analysis, a probability density function of acquired Von Mises stresses is produced assuming the lognormal distribution. It is based on histogram shape. *Pdf* is calculated with respect to mean value and standard deviation. Lognormal distribution's logarithm is normally distributed. Such distribution has only positive random variables X, and a non-symmetry (skewness) as in histogram case, so it appeared convenient here. *Pdf* of stress (Von Mises stress or just stress, X is random variable) and statistical parameters are shown in eq. (2) while original equations are taken from reference by O'Connor and al. (2016). They include: mean (μ) and standard deviation (σ) of stresses obtained from Table 1 and their corresponding mean (μ_N) and standard deviation (σ_N) of the normally distributed ln(X). Lognormal pdf is presented in Fig. 3. (b).

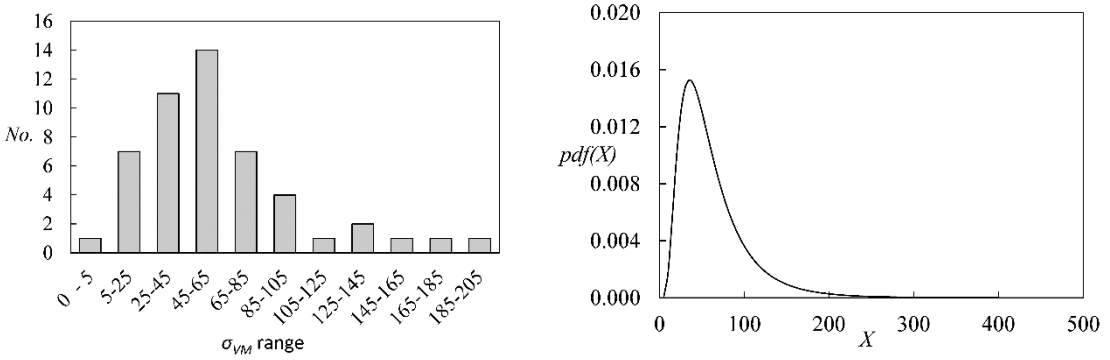

Fig. 3. (a) Von Mises Stress histogram, (b) Von Mises Stress lognormal probability density function

$$pdf(X) = \frac{1}{\sigma_N X \cdot \sqrt{2\pi}} \exp\left[-0.5 \cdot \left(\frac{\ln(X) - \mu_N}{\sigma_N} \right)^2 \right]$$

$$\mu = \frac{\sum_{i=1}^{n} X_i}{n} = 62.09\,MPa \qquad \sigma^2 = \frac{\sum_{i=1}^{n} (X_i - \mu)^2}{n} \rightarrow \sigma = \sqrt{\sigma^2} = 41.78\,MPa \tag{2}$$

$$\mu_N = \ln\left(\frac{\mu^2}{\sqrt{\sigma^2 + \mu^2}} \right) = 3.94\,MPa \qquad \sigma_N^2 = \ln\left(\frac{\sigma^2 + \mu^2}{\mu^2} \right) \rightarrow \sigma_N = \sqrt{\sigma_N^2} = 0.61\,MPa$$

3.2. Criterion

Criterion includes a yield limit of the structure material, i.e., mild steel – S355. In practice, a so called "safety factor (SF)" of 1.5 is used with respect to the yield limit (355 MPa), see German National Standard, DIN 22261-2. Therefore, a criterion is derived to be 236.67 MPa (355 MPa/1.5). Note that in the paper, a label "safety factor (SF)" will be used

when evaluating the difference between the criterion and stress distributions, while a "reduction factor (RF)" will be applied to account the ratio between the actual criterion and the stresses. Mean value and standard deviation of the S355 yield distribution is taken from reference by Sadowski et al. (2014). Yield limit pdf is assumed as normally distributed, which is mostly accounted in literature. Mean value of reduced criteria (for RF < 1) is determined as in eq. (3). Consequently, various *pdfs* of allowable stress (as portion of yield limit distribution), are produced using eq. (4), as shown in Fig. 4. Furthermore, authors analyzed the effect of RF variation, since structural engineer is often changing the evaluation criterion in order to gain more structural safety, see Table 2. Then, for each of the RF, a reliability and reliability index are calculated.

$$\mu(\sigma_{all,i}) = RF_i \mu(\sigma_y) \qquad \sigma(\sigma_{all,i}) = const. \tag{3}$$

$$pdf(X) = \frac{1}{\sigma\sqrt{2\pi}} \exp\left[-0.5 \cdot \left(\frac{X-\mu}{\sigma}\right)^2\right], \quad \mu = \frac{\sum_{i=1}^{n} X_i}{n}, \quad \sigma^2 = \frac{\sum_{i=1}^{n} (X_i - \mu)^2}{n} \rightarrow \sigma = \sqrt{\sigma^2} \tag{4}$$

Table 2. Statistical properties of the criteria.

σ_y[MPa]	σ_y/σ_{all}	σ_{all} [MPa]	RF = σ_{all}/σ_y	μ	σ	$\sigma_{all,min}$ [MPa]	$\sigma_{all,max}$ [MPa]
355	1	355.00	1.00	405.70	69.1	350	602
355	1.5	236.67	0.67	270.47	69.1		
355	2	177.50	0.50	202.85	69.1		
355	3	118.33	0.33	135.23	69.1		
355	4	88.75	0.25	101.43	69.1		
355	5	71.00	0.20	81.14	69.1		

4. Margin Function and Monte Carlo Simulation

Both Von Mises stress (from sect. 3.1) and allowable stress (from sect. 3.2) are plotted with their *pdfs*, as in Fig. 4. Area in which the capacity and demand functions are overlapping is representing the failure of the limit state function M. In such cases, the demand could be larger than the capacity producing M < 0 (see shaded area in Fig. 4. (a)) when comparing yield distribution having RF = 0.67 and stress distribution). The probability of failure Pf is defined as in eq. (5), where $f(\sigma_{VM}, \sigma_{all})$ is called a joint probability density function (*jpdf*) of the both Von Mises and allowable stress domain.

$$P_f(M = C - D < 0) = \iint_{C-D<0} f(\sigma_{VM}, \sigma_{all}) dx dx \qquad P_f \approx \frac{n(M<0)}{N} \qquad R = 1 - P_f \tag{5}$$

In order to calculate area of the *jpdf* in which M < 0, a Monte Carlo simulation is used. During such procedure, the 10000 random number sets are produced in accordance with probability distributions of known Von Mises stress and allowable stress for various RFs. Random number sets that satisfied M = C – D < 0 are counted and divided by the number of sets totally produced, to obtain probability of failure P_f. Moreover, the reliability is calculated as 1-P_f, see also eq. (5).

Moreover, the safety margin (SM) is calculated as a relative difference between the mean values of the allowable stress and Von Mises stress pdfs. Nonetheless, mean of margin M is the difference between mean values of the capacity and demand, i.e., allowable and Von Mises stress distributions. Standard deviation of M is calculated based on standard deviations of both pdfs, and also taking into account the correlation between two distributions. For the purpose of this analysis, a correlation coefficient is assumed as being ρ=0 meaning that the distributions are uncorrelated. Finally, reliability index β, as a measure of safety and structural performance of the object, is calculated as ratio between mean and standard deviation of margin M. Procedure for abovementioned particulars is given in eq. (6) and based on equations given in reference by Choi et al. (2007). The results are shown in Table 3 and Fig. 4.

$$SM = \frac{\mu(\sigma_{VM}) - \mu(\sigma_{all})}{\left(\sigma^2(\sigma_{all}) + \sigma^2(\sigma_{VM})\right)^{0.5}} \qquad \mu(M) = \mu(\sigma_{VM}) - \mu(\sigma_{all})$$
$$\sigma(M) = \sqrt{\sigma^2(\sigma_{all}) + \sigma^2(\sigma_{VM}) - 2\rho\sigma(\sigma_{all})\sigma(\sigma_{VM})} \qquad \beta = \frac{\mu(M)}{\sigma(M)} \tag{6}$$

Table 3. Statistical properties of the margin M.

	Stress (D)	Allowable stress (D)					
RF	1.00	1.00	0.67	0.50	0.33	0.25	0.20
μ	62.09	405.70	270.47	202.85	135.23	101.43	81.14
σ^2	1745.10	4774.81	4774.81	4774.81	4774.81	4774.81	4774.81
SM		4.26	2.58	1.74	0.91	0.49	0.24
μ(M)		343.61	208.38	140.76	73.15	39.34	19.05
σ(M)		80.75	80.75	80.75	80.75	80.75	80.75
P_f		0.003	0.022	0.060	0.189	0.312	0.397
R		0.997	0.978	0.940	0.811	0.688	0.606
β		4.26	2.58	1.74	0.91	0.49	0.24

If criterion is presented by an actual yield limit, the probability of failure is negligible, the reliability is high and almost equal to 1 and the reliability index is large (4.26), meaning that the structure is safe considering inputs. The structure can be also labelled as relatively safe when current practice from design codes (RF = 0.67) are taken into account. However, soon below the RF = 0.6, the structure tends to deliver much higher probabilities of failure and therefore, be less reliable. The trend is not linear. So, the choice of RF should be evaluated carefully when lower allowable stresses are considered.

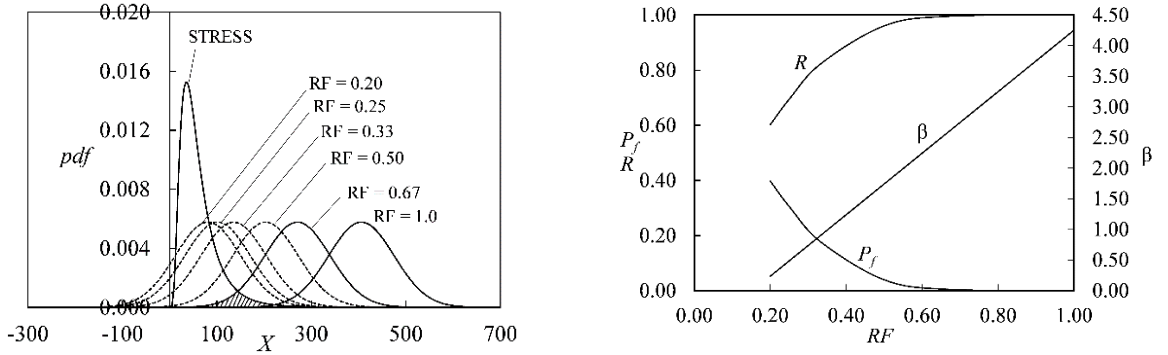

Fig. 4. (a) Von Mises stress and allowable stress probability density functions, (b) Reliability, reliability index, probability of failure

5. Conclusion

The paper introduces the reliability-based analysis of the bucket wheel excavator's load-bearing steel structure. The analysis here is different from the general found in literature since the reliability is assessed with respect to the "just" structural response. Von Mises stresses are compared to the yield limit in terms their respective probability density distributions, which is considering their uncertainties. For each of the failure criteria, authors quantified the level of failure, reliability and furthermore delivered reliability index. Analysis is not based on historical data obtained for the structure. It is rather a "design – based" reliability evaluation performed using stresses as random variables. However, one can argue that there are many other ways to consider reliability of such structures. Authors did not take into account the failure of mechanical systems or the influence of other, minor type, loading conditions. Furthermore, the criterion is based on yield limit. Despite, some of structural members may experience buckling collapse rather than yielding. Moreover, the proposed stress distribution is, to some extent, favoring the maximum stress rather than the lower values.

Acknowledgements

This work is supported by the Ministry of Science and Technological Development of Serbia (no. 451-03-9/2021-14/200105)

References

Melchers, R. E., Beck, A. T., 2018. Structural Reliability Analysis and Prediction, 3rd edition. John Wiley & Sons Ltd.

Wang, C., 2021. Structural Reliability and Time-Dependent Reliability. Springer.

Kovač, N., Ivošević, Š., 2022. Reliability of corrosion depth database for alloys exposed to the marine environment, Structural Integrity and Life, 22(1), 3-17

Nguyen, T.H., Le, H.X., 2019. A Practical Method for Calculating Structural Reliability with a Mixture of Random and Fuzzy Variables, Structural Integrity and Life, 19(3), 173-185

Sedmak, S.A., Arsić, M., Bošnjak, S., Malešević, Z., Savić, Z., Radu, D., 2016. Effect of Locally Damaged Elbow Segments on the Integrity and Reliability of the Heating System, Structural Integrity and Life, 16(3), 167-170

Kalaba, D., Đorđević, M., Kirin, S., Delamarian, C., 2016. Determining Reliability Functions of Steam Turbine in Power Plant 'Nikola Tesla, Block A4', Structural Integrity and Life, 16(1), 9-13

Kalaba, D., Đorđević, M., Ivanović, V., 2015. Determining the Reliability Functions of the Boiler Tubing System in Power Plant 'Nikola Tesla, Block A4', Structural Integrity and Life, 15(3), 167-171

Ristić, M., Ognjanović, M., 2014. Integrity of Gear Transmission Units Indicated by Reliability for Design, Structural Integrity and Life, 14(3), 167-170

Novoselac, S., Kozak, D., Ergić, T., Damjanović, D., 2014. Fatigue Damage Assessment of Bolted Joint Under Different Preload Forces and Variable Amplitude Eccentric Forces for High Reliability, Structural Integrity and Life, 14(2), 93-109

Szávai, S., Köves, T., 2010. Reliability and Lifetime Analysis for a Cracked Cylinder of Ammonia Unit Compressor, Structural Integrity and Life, 10(3), 187-192

Arsić, M., Flajs, Ž., Sedmak, A., Veg, E., Sedmak, S., 2021. Structural integrity assessment of welded bucket-wheel boom, Structural Integrity and Life, 21(2), 201-206

Daničić, D., Sedmak, S., Blačić, I., Kirin, S., 2013. Scenario of Fracture Development in Bucket Wheel Excavator, Structural Integrity and Life, 13(2), 189-196

Daničić, D., Maneski, T., 2012. The Structure Failure of the Discharge Boom of Bucket Wheel Excavator C 700 S due to Dynamic Effects, Structural Integrity and Life, 12(1), 43-46

Polovina, D., Ivković, S., Ignjatović, D., Tanasijević, M., 2010. Remaining operational capabilities evaluation of bucket wheel excavator by application of expert assessment method with empirical correction factor, Structural Integrity and Life, 10(1), 31-41

Tanasijević, M., Ivezić, D., Jovančić, P., 2010. Estimation of bucket wheel excavator dependability using fuzzy algebra rules, Structural Integrity and Life, 10(1), 43-52

Daničić, D., Maneski, T., Ignjatović, D., 2010. Structural diagnostics and behaviour of bucket wheel excavatorDaničić et al (2010), Structural Integrity and Life, , 10(1), 53-59

Arsić, M., Aleksić, V., Radaković, Z., 2008. The effect of residual stresses in welded joint on the failure of bucket wheel excavator, Structural Integrity and Life, 8(1), 13-22

Lazarević, Ž., Arandjelović, I., Kirin, S., 2015. An Analysis of Random Mechanical Failures of Bucket Wheel Excavator, Structural Integrity and Life, 15(3), 143-146

Lazarević, Ž., Arandjelović, I., Kirin, S., 2018. The Reliability of Bucket Wheel Excavator - Review of Random Mechanical Failures. Technical Gazette, 24(4), pp. 1259-1264.

Tomus, O. B., Andras, A., Jula, D., Dinescu, S., 2019. Aspects relating to the reliability calculation of the cutting-teeth mounted on the bucket wheel excavators used in lignite mining, 9th International Conference on Manufacturing Science and Education – MSE 2019.

Petrović, A., Ignjatović, D., Sedmak, S., Milošević-Mitić, V., Momčilović, N., Trišović, N., Jeremić, L., 2021. Model analysis of bucket wheel excavator SchRs 630 strength. Engineering Failure Analysis, Vol. 126.

Maneski, T., 1998. Computer Modeling and Calculation of Structures, Faculty of Mechanical Engineering, Belgrade, (in Serbian).

O'Connor, A. N., Modarres, M., Mosleh, A., 2016. Probability Distributions Used in Reliability Engineering, Center for Risk and Reliability - University of Maryland.

Motok, M., Momčilović, N., Rudaković, S., 2022. Reliability based structural design of river–sea tankers: Still water loading effects. Marine Structures, Vol. 83.

Deutsches Institut Fur Normung E.V. (DIN) - German National Standard, DIN 22261-2: Excavators, spreaders and auxiliary equipment in opencast lignite mines - Part 2: Calculation principles, standard, pp 116, 2016.

Sadowski, A.J., Rotter, J.M., Reinke, T., Ummenhofer, T., 2014. Statistical analysis of the material properties of selected structural carbon steels. Structural Safety, 53C, pp 26-35.

Choi, S. K., Grandhi, R. V., Canfield, R. A., 2007. Reliability-based Structural Design. Springer.